

Characterization and Application of a Nose-Only Exposure Chamber for Inhalation Delivery of Liposomal Drugs and Nucleic Acids to Mice

G. Mainelis, PhD,¹ S. Seshadri, PhD,¹ O.B. Garbuzenko, PhD,² T. Han, PhD,¹
Z. Wang, PhD,¹ and T. Minko, PhD²

Abstract

Background: A small nose-only exposure chamber was evaluated for inhalation delivery of drug carrier systems (DCSs) to mice for the treatment of lung cancer. The chamber then was used for inhalation delivery of an anticancer drug, antisense oligonucleotides (ASO), and small interfering RNA (siRNA) directly to the cancerous lungs of mice.

Methods: The uniformity of particle delivery across the ports of the exposure chamber and stability of the DCS (liposomes) during continuous aerosolization by a Collison nebulizer were examined. The mean produced particle size by number was approximately 130 nm, and the mass median diameter was approximately 270 nm. The system was then used to deliver DCS containing doxorubicin (DOX) and ASO or siRNA targeted to multidrug resistance-associated protein 1 (MRP1) mRNA as suppressors of cancer cell resistance. The retention of the drug in the lungs and the effect on tumor size were compared after inhalation delivery and intravenous injection in a nu/nu mouse model of lung cancer.

Results: The aerosol mass across the four inhalation ports had a coefficient of variation of less than 12%, and approximately 1.4% of the nebulized mass was available for inhalation at each port. The mean size of 130 nm of liposomal DCS did not change significantly during continuous 60-min aerosolization. For inhalation delivery of DCS with DOX + ASO/siRNA, the amount of drugs available for inhalation was lower compared with intravenous injection of DOX; however, the observed lung dose and the retention time were significantly higher. The delivery of DOX + ASO/siRNA via inhalation resulted in tumor volume reduction of more than 90%, whereas only about 40% reduction was achieved after intravenous injection of DOX.

Conclusions: The investigated exposure system is suitable for inhalation delivery of complex DCS, and its use to deliver DCS containing anticancer drugs and resistance suppressors via inhalation offered a superior method for lung cancer treatment in mice compared with intravenous injections.

Key words: lung cancer, inhalation, exposure, nose-only chamber, drug carrier systems, liposomes, pump and nonpump resistance

Introduction

LUNG CANCER IS CONSIDERED to be the leading cause of cancer-related death around the world,⁽¹⁾ resulting in 1.18 million deaths per year.⁽²⁾ Once the lung cancer becomes developed, its surgical removal is often not very effective due to its size and wide dissemination, which leaves chemotherapy and/or radiation as treatments of choice. The success of che-

motherapeutic treatment of small-cell lung cancer, a more aggressive type compared with non-small-cell lung cancer, is limited by the intrinsic and acquired resistance of cancer cells to chemotherapy. The main mechanisms of this resistance are common to most cancers and include “pump” and “non-pump” resistance.^(3,4) The pump resistance is caused by membrane transporters that pump out the anticancer agents from cells, decreasing the intracellular drug concentration and

¹Department of Environmental Sciences, Rutgers, The State University of New Jersey, New Brunswick, NJ 08901.

²Department of Pharmaceutics, Rutgers, The State University of New Jersey, Piscataway, NJ 08854.

thereby the efficacy of the treatment. The main mechanism of nonpump resistance is the activation of the cellular anti-apoptotic defense. Currently, to overcome this resistance, high doses of toxic anticancer drug(s) are administered, often producing adverse side effects in healthy organs. Recently, we demonstrated that the efficacy of the chemotherapy can be substantially enhanced if both resistance mechanisms are simultaneously suppressed when an anticancer agent(s) is delivered.⁽³⁻⁵⁾ We also showed that antisense oligonucleotides (ASO) and small interfering RNA (siRNA) can be efficiently used to suppress both types of resistance.⁽⁶⁻⁸⁾ However, ASO and siRNA poorly penetrate cancer cells, are unstable in the bloodstream, and therefore require a special carrier system to preserve their activity in the extracellular environment and increase their accumulation in cancer cells. On the other hand, the treatment could be enhanced and its severe adverse side effects avoided if the anticancer drugs combined with ASO or siRNA were delivered not to the entire body via injection or ingestion, but only to the affected lungs via inhalation. Inhalation is considered a rational route to deliver drugs against lung cancer; however, relatively few drugs have been investigated.⁽⁹⁾

A local drug delivery, including inhalation delivery of the drugs to lungs, offers several substantial advantages, including simplified administration protocol, reduced drug quantity needed to achieve therapeutic effect, and increased drug concentration at the required sites.⁽¹⁰⁾ The inhalation of certain drugs was suggested as early as 1946, when the description of a nebulizer for penicillin was published.⁽¹¹⁾ When it comes to anticancer drugs, inhalation delivery would enhance the accumulation of anticancer agent(s) in the lungs with tumor and reduce severe toxic side effects on healthy tissues.⁽⁵⁾

Inhaled drugs are commonly used by patients with asthma and chronic obstructive pulmonary disease.⁽¹²⁾ Although some chemotherapeutic agents can be delivered through the pulmonary or intratracheal route,⁽¹³⁻¹⁶⁾ most anticancer drugs, as well as resistance suppressors ASO and siRNA, cannot be inhaled in their traditional form and require a special drug carrier system (DCS). Several different DCSs have been recently developed for the inhalation delivery of different drugs; among those, lipid and polymer-based nanoparticles⁽¹⁷⁻²⁰⁾ and liposomes⁽²¹⁻²⁵⁾ are the most frequently used carriers for local pulmonary delivery.

Liposomes have been widely investigated since 1970 as drug carriers for improving the delivery of therapeutic agents to specific sites in the body, and almost immediately were explored for cancer treatment.^(26,27) When the liposomes are administered systemically, their residence time in the circulatory system is short due to elimination by the reticuloendothelial system, which limits their therapeutic application.^(28,29) In contrast, delivery of liposomal drugs via inhalation increases drug retention time in the lungs^(5,25) and reduces extrapulmonary side effects.^(5,30) Consequently, delivery of anticancer agent(s) together with suppressor(s) of cancer cell resistance in one DCS directly to the lung via inhalation would be capable of substantially enhancing the efficacy of the treatment of lung cancer and limiting the adverse side effects of chemotherapy on healthy organs. This approach is the focus of our ongoing study, and substantial progress and encouraging results have already been reported in an animal (mouse) model.^(5,25)

Once a suitable DCS, such as liposomes, is developed and prepared to carry out *in vivo* testing, it has to be aerosolized and delivered to test animals for inhalation exposure in a way that does not affect the efficacy of its active ingredients. As an aerosolization method could potentially affect the integrity of the DCS, as well as its airborne number and mass distributions, these variables have to be explored before the actual animal exposures can begin. In addition, the drug delivery and exposure system itself has to be characterized to estimate the inhaled dose and to ensure that all test animals receive comparable doses of the DCS.

The animals in pharmaceutical or inhalation toxicology studies are usually exposed using whole-body exposure chambers or nose-only and head-only systems for single or multiple animals.⁽³¹⁾ In this study, we used a directed-flow, nose-only exposure system, because systems of this type eliminate the potential dilution of exposure air by the exhaled air of other animals.⁽³¹⁾ A five-port nose-only exposure chamber manufactured by CH Technologies Inc. (Westwood, NJ) was used to expose mice to the therapeutics. This five-port design is based on its better-known cousin "12 port nose-only modular system," which can be stacked in tiers in up to four layers, from the same manufacturer. This system uses a flow-past design⁽³²⁾ to minimize variation in the concentration of aerosols delivered at the exposure port. The 12-port system has been characterized and used in several studies.⁽³³⁻³⁵⁾ Although the five-port system has the same basic design for aerosol distribution, it has been substantially modified compared with the 12-port model, warranting its separate characterization before the exposure experiments could commence. Thus, the main goal of this project was to determine the size distribution and stability of aerosolized DCS, analyze the five-port exposure system, and then apply the system for actual delivery of the DCS *in vivo*. These efforts are described below.

Materials and Methods

Exposure system

Figure 1A shows the top view of the five-port animal exposure system (CH Technologies), including the aerosol distribution chamber and animal containment tubes numbered from P1 through P5, whereas Figure 1B shows the cross-sectional view of the exposure system along with aerosol generation and measurement devices. The cross-sectional view in Figure 1B corresponds to the AA line in Figure 1A.

During our experiments, the test particles were aerosolized using a one-jet Collison nebulizer (BGI Inc., Waltham, MA) operated at an aerosolization flow rate $Q_{\text{COLL}} = 2 \text{ L/min}$ using dry [relative humidity (RH) = 0%] and purified air (Airgas East, Salem, NH). The Collison nebulizer was equipped with a precious fluid cup to minimize the amount of liquid needed for reliable aerosolization. The aerosolized liquid droplets were diluted and desiccated using dry (RH = 0%) and purified air (Airgas East) at a dilution flow rate $Q_{\text{DIL}} = 2 \text{ L/min}$. Then, under a slight positive pressure (0.1" w.g.), the entire aerosol flow entered a mixing box of the distribution chamber and was distributed to each animal containment tube via round pipes. Each containment tube is connected to the distribution chamber via a connector cone, which features a spout in its middle to deliver fresh aerosol

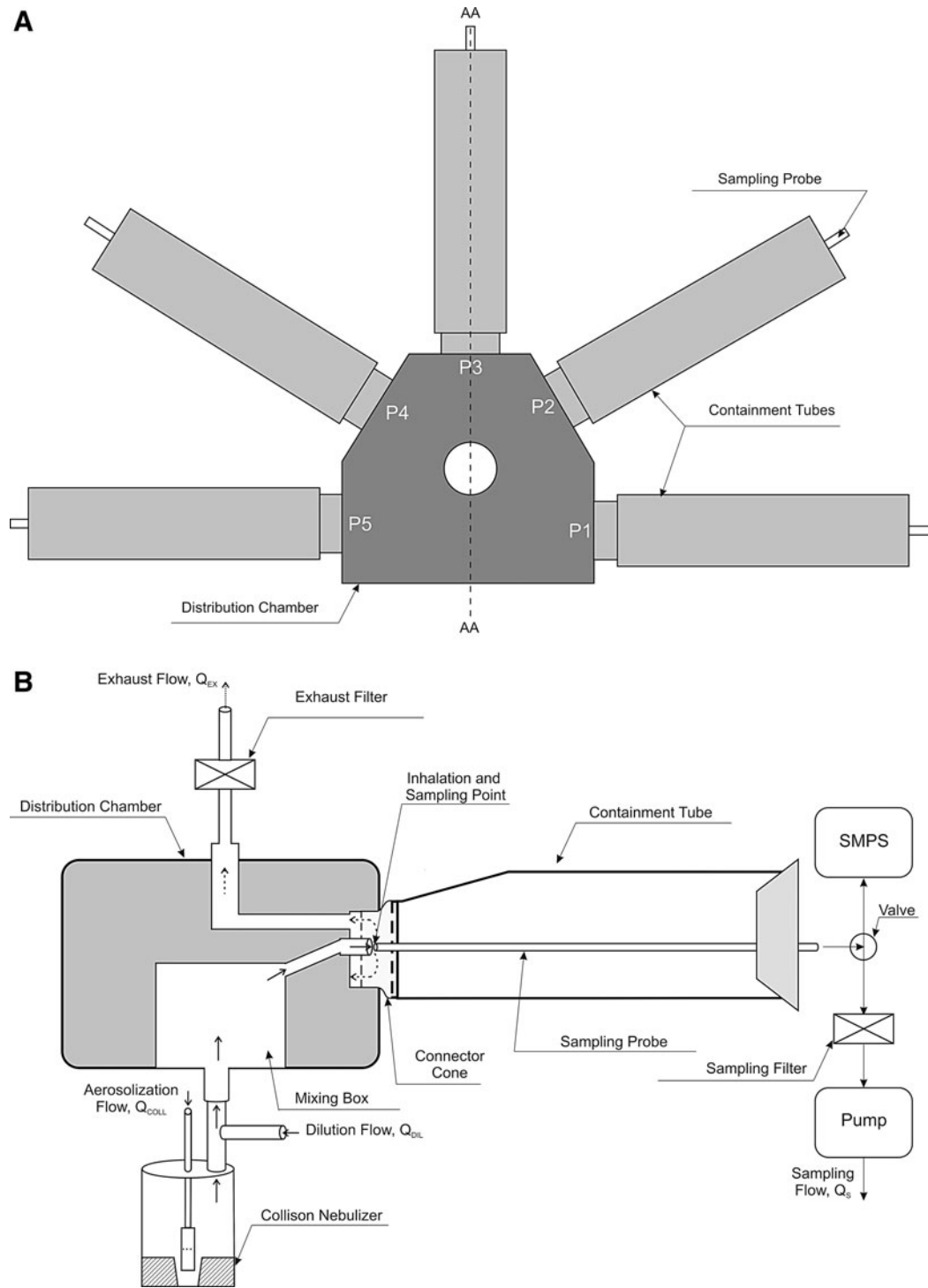


FIG. 1. (A) Schematic of the exposure chamber, including the aerosol distribution chamber and the mouse containment tubes. Details of the distribution chamber along the line AA are shown in (B). The drawing is not to scale. (B) Schematic of the experimental setup showing the cross-sectional view of the exposure system along with aerosol generation and measurement devices. Solid arrows in the distribution chamber indicate fresh aerosol, and dotted arrows indicate the exhausted aerosol. The drawing is not to scale.

to a test animal and round openings in its back for exhaled air. During the inhalation experiments, each test animal is positioned in a containment tube so that the animal's nose is at the spout, or "inhalation point." The animal is held in place by a plunger. The air exhaled by the test animal es-

capates the connector cone via openings in the cone's back and is exhausted. The air exhausted from all containment tubes is gathered at a common exhaust line, passes through a filter, and leaves the exposure system at a flow rate $Q_{EX} = Q_{COLL} + Q_{DIL} = 4 \text{ L/min}$. As the containment tube is airtight

and sealed by a rubber plug, no air enters or leaves the exposure system except via the aerosol delivery and exhaust. To prevent potential exposure of the study personnel to the test particles, the entire exposure system was housed in a Class II biosafety cabinet (NUAIRE Inc., Plymouth, MN). Two identical aerosol distribution chambers were tested and are denoted as Chambers A and B in the Results section.

During the characterization of the exposure system, no animals were placed in the containment tubes, but instead the sampling probes (Figure 1B) were inserted to sample the air from approximately the same point where an animal's nose would be. The aerosol was sampled at the "inhalation point" and collected either on a filter or measured using a direct reading aerosol instrument as described below. Although the exposure chamber is designed to house five test animals, the exposure protocol called for the use of four test animals at a time; therefore, port P3 was sealed with a black rubber stopper.

Test particles

The initial characterization of the exposure chamber was performed with green fluorescent polystyrene latex (PSL) particles (Duke Scientific, Palo Alto, CA) of 0.2, 0.5, and 1.2 μm in size. Once the performance of the system was examined with PSL particles, it was further tested with actual DCS (nanoscale liposomes) designed to contain the following: doxorubicin (DOX) as a cell death inducer, and either p-ethoxy-modified ASO or siRNA targeting multidrug resistance-associated protein 1 (MRP1) mRNA as a suppressor of pump resistance and BCL2 mRNA as a suppressor of nonpump resistance. The liposomes used to deliver ASO were electrically neutral. They were prepared in-house as previously described⁽²⁵⁾ and consisted of egg phosphatidylcholine:1,2-dipalmitoyl-*sn*-glycero-3-phosphatidylcholine:cholesterol at a ratio of 7:3:10. Negatively charged siRNA was delivered by cationic 1,2-dioleoyl-3-trimethylammonium-propane (DOTAP) liposomes.⁽²⁵⁾ To analyze the liposome mass distribution across different exposure ports of the exposure system, liposome types were labeled with either near-infrared fluorescent dye Cy5.5 Mono NHS Ester (GE Healthcare, Amersham, UK) or fluorescein isothiocyanate (FITC), as previously described.⁽²⁵⁾ Initial concentrations of both types of liposomes in liquid were 5 mg/mL. Before aerosolization, both suspensions were diluted to 1 mg/mL concentration.

Analysis of liposome stability

Pneumatic aerosol nebulizers, such as the Collison nebulizer used in this study, are known to exert considerable shear forces on the particles being aerosolized.⁽³⁶⁾ In addition, the liquid in the device is constantly recirculated, which could lead to the accumulation of stress during the prolonged nebulization. At high pressures and prolonged usage, the stress can lead to the loss of particle integrity.^(37,38) Thus, to ensure that the integrity of the DCS is not affected during exposure experiments, the Collison nebulizer was operated continuously for 60 min at a low pressure of 20 psi, and size distributions of airborne and liquid-borne liposomes were examined before and after nebulization. The airborne liposome size distribution was monitored every 15 min using a Scanning Mobility Particle Sizer[®] (SMPS) (model 3936; TSI Inc., Shoreview, MN), which samples air at 0.3 L/min and

determines particle electrical mobility diameter from 14 to 700 nm (Fig. 1B). The size of the liquid-borne liposomes was analyzed using photon correlation spectroscopy using Zeta-PALS 90 Plus with particle sizing software (Brookhaven Instruments Corporation, Holtsville, NY), which determines hydrodynamic particle diameter. The latter accounts for the electric double layer around a particle and represents the diameter of a hypothetical sphere that would diffuse at the same rate as the particle under examination.

During the initial experiments, the produced aerosol was also characterized using an Aerodynamic Particle Sizer[®] (APS) (model 3321; TSI Inc.) in parallel with the SMPS. The APS (not shown in Fig. 1B) measures the aerodynamic diameter of the particles ranging from 0.5 to 20 μm . However, based on the obtained data (described in Results), this device was not used in further experiments.

Analysis of the aerosol mass distributions across different exposure ports

One of the key attributes of any exposure system is the ability to expose all test animals to approximately the same concentration of test aerosol. In addition, day-to-day experiments should also produce similar exposures. Prior to testing the mass distributions across the ports with the DCS, a series of experiments was performed with airborne fluorescent PSL particles of different sizes. Here, a probe was inserted into each containment tube so that a probe's inlet would be in approximately the same position as an animal's nose. The air flow of $Q_s = 25 \text{ mL/min}$ through each probe was provided by a pump with a low-flow adapter (SKC Inc., Eighty Four, PA), and the particles were collected on an A/E glass fiber filter with 1.0- μm pore size (Pall Inc., East Hills, NY) positioned immediately after the containment tube (Fig. 1B). In addition, particles exiting the exposure chamber were collected on an exhaust filter of the same type. The four probes at ports P1, P2, P4, and P5 were operated simultaneously. The relative mass concentration of PSL particles collected on each filter was quantified by a fluorometer (FM109515; Sequoia-Turner Corp., Mountain View, CA) using a procedure described elsewhere.⁽³⁹⁾ In brief, each filter with collected particles was soaked in 25 mL of ethyl acetate in a glass container for 4 hr to elute the fluorescein dye from the PSL particles, and then an aliquot of 100 μL was used to measure fluorescence intensity from each sample. Using the data from the five filters, the following two parameters were calculated: aerosol mass fraction at each exposure port relative to the aerosol mass collected on all filters (four ports and exhaust): η_{Ti} . We also determined the aerosol mass fraction at each exposure port relative to the aerosol mass collected at four ports, η_{Pi} . The η_{Pi} was calculated as a ratio of fluorescence intensity, I_i , on a particular filter recorded by the fluorometer relative to the sum of intensities on all four filters from the exposure ports; to calculate the η_{Ti} , the fluorescence intensity on the exhaust filter, I_{EX} , was added to the denominator:

$$\eta_{Pi} = \frac{I_i}{\sum_i I_i}; \quad \eta_{Ti} = \frac{I_i}{\sum_i I_i + I_{EX}} \quad (1)$$

The η_{Pi} indicates whether the mass concentration across the four ports is uniform. The η_{Ti} indicates what fraction of the

total aerosol is delivered to an inhalation point and could potentially be inhaled by a test animal, assuming aerosol losses inside the exposure chamber are minimal. For the sizes of the tested particles and their velocities in the exposure system, the particles' Stokes number as well as their diffusion coefficient is low, indicating that particle losses would be minimal. The η_{Ti} is important for repeated exposures when the same aerosolization parameters are used.

The concentration of aerosolized PSL particles was such as to ensure that the fluorometer reading of each sample was approximately 10-fold of the background fluorescence of ethyl acetate, and the measurements were adjusted for background readings. In addition, the concentrations of all analyzed samples were within the linearity range of the fluorometer.

When analyzing the mass distribution of liposomes across the exposure ports, we used fluorescently tagged liposomes, and the measurement procedure was the same as for the PSL particles, except that ethanol was used to extract the fluorescent dye.

In addition, we determined the relationship between various concentrations of fluorescently tagged liposomes in liquid (in milligrams per milliliter) and their produced fluorescence intensity units (FIU). The mass of liposomes collected on the filters at exposure ports was determined by soaking each filter in 25 mL of alcohol, measuring the resulting FIU, and using the calibration curve.

Application of the system for in vivo tumor growth and treatment

Nude nu/nu mice, 6–8 weeks old, were purchased from Taconic (Hudson, NY). An A549 human lung adenocarcinoma epithelial cell line transfected with luciferase was purchased from Xenogen Corporation (Alameda, CA). Cancer cells ($5\text{--}6 \times 10^6$) were resuspended in 0.1 mL of Roswell Park Memorial Institute medium containing 20% fetal bovine serum, mixed with $5\ \mu\text{mol}$ of ethylenediaminetetraacetic acid, and administered to the mouse lung through a catheter. Rapid growth of lung tumor developed in 80% of animals.⁽⁵⁾ The progression of tumor growth was monitored by a bioluminescent IVIS imaging system (Xenogen Corporation). The calibration data are presented elsewhere.⁽⁵⁾

Four weeks after the instillation of tumor cells, groups of mice were treated on days 0, 3, 7, 11, 14, 17, 21, and 24 with one of the following drug formulations: (a) intravenous (i.v.) injection of saline in untreated mice as control; (b) free DOX via i.v. injection (i.v.-DOX); (c) liposomal DOX via i.v. injection [i.v.-Lip(DOX)]; (d) liposomal DOX via inhalation [inh-Lip(DOX)]; (e) liposomal ASO-FITC via i.v. [i.v.-Lip(ASO-FITC)]; (f) liposomal ASO-FITC via inhalation [inh-Lip(ASO-FITC)]; and (g) inhalation of a complex liposomal DCS containing DOX, MRP1, and BCL2 ASO [inh-Lip(DOX+ASO)]. There were eight mice in each treatment group. Inhalation administration was performed with the exposure system under investigation, and each inhalation exposure consisted of inhaling room air for 5 min (to allow the mice to calm down) and then inhalation treatment of 10 min.

The concentration of DOX injected both as the free DOX (i.v.-DOX) and as liposomal DOX [i.v.-Lip(DOX)] was $50\ \mu\text{g}/100\ \mu\text{L}$. One hundred microliters was injected in each application, and it

resulted in a DOX dose of $2.5\ \text{mg}/\text{kg}$ per each i.v. application for a 20-g mouse. This dose corresponds to the maximum tolerated dose (MTD) of free DOX (i.v. injection). The MTD of free DOX was estimated in separate experiments based on animal weight change after the injection of increasing doses of DOX, as previously described.^(40,41) The applied DOX dose was not observed to cause significant side effects, and very low levels of apoptosis induction were registered in healthy organs.⁽⁵⁾ The concentration of ASO in liquid was $2.5\ \mu\text{g}/100\ \mu\text{L}$, which yielded the ASO dose of $0.125\ \text{mg}/\text{kg}$ per i.v. application. The concentration of lipids in the nebulizer solution was $5\ \text{mg}/\text{mL}$. For inhalation, the concentration of DOX and ASO in the nebulizer solution was the same as in i.v. solution, i.e., $50\ \mu\text{g}/100\ \mu\text{L}$ and $2.5\ \mu\text{g}/100\ \mu\text{L}$, respectively. The resulting inhalation dose was estimated based on the experiments with fluorescent liposomes and fluorescent PSL particles. In the latter experiments, the collection flow rate at each exposure port was $0.025\ \text{L}/\text{min}$, and the particles were nebulized and collected for 10 min. The concentration of $0.2\text{-}\mu\text{m}$ PSL particles in the liquid was $40\ \mu\text{g}/100\ \mu\text{L}$, i.e., similar to that of DOX. The estimate of inhaled dose is provided in Results. For each application type, the drug concentrations and the resulting doses were the same during all application days.

Once the treatment was completed, the accumulation and retention of DOX and ASO in the lungs and total volume of lung tumor were measured using the IVIS imaging system (Xenogen Corporation), as previously described.^(5,25) The initial tumor volume in all mice was approximately $40\ \text{mm}^3$.

Statistical analysis

The obtained data were analyzed using descriptive statistics, single-factor analysis of variance (ANOVA), and presented as a mean value \pm standard deviation (SD) from five (*in vitro*) or eight (*in vivo*) independent measurements. We analyzed data sets for significance with Student's *t* test and considered *p* values of less than 0.05 as statistically significant.

Results and Discussion

Figure 2 presents the relative aerosol mass fraction η_{Pi} across four ports obtained with the fluorescent PSL particles. As can be seen, the relative mass fraction did not vary substantially across exposure ports of both chambers. For Chamber A, the mass fractions ranged from 0.23 to 0.28 for $0.2\text{-}\mu\text{m}$ PSL, from 0.21 to 0.27 for $0.5\text{-}\mu\text{m}$ PSL, and from 0.23 to 0.29 for $1.2\text{-}\mu\text{m}$ PSL. For Chamber B, the mass fractions ranged from 0.23 to 0.26 for $0.2\text{-}\mu\text{m}$ PSL, from 0.22 to 0.29 for $0.5\text{-}\mu\text{m}$ PSL, and from 0.22 to 0.27 for $1.2\text{-}\mu\text{m}$ PSL.

According to one-way ANOVA test, the mass fractions across four exposure ports of both chambers in almost all cases did not differ significantly for different PSL sizes ($p > 0.05$). One exception was the distribution of $0.5\text{-}\mu\text{m}$ PSL across the ports of Chamber A, where the difference was statistically significant ($p < 0.02$). The Bonferroni pairwise comparisons among the ports of Chamber A showed that there were statistically significant differences between ports P1 versus P2 and P2 versus P5 for $0.5\text{-}\mu\text{m}$ PSL particles. However, when the data for different PSL particle sizes were pooled, the Bonferroni pairwise comparisons did not show statistical difference among the four ports. For Chamber B, there was a statistical difference between ports P1 and P2

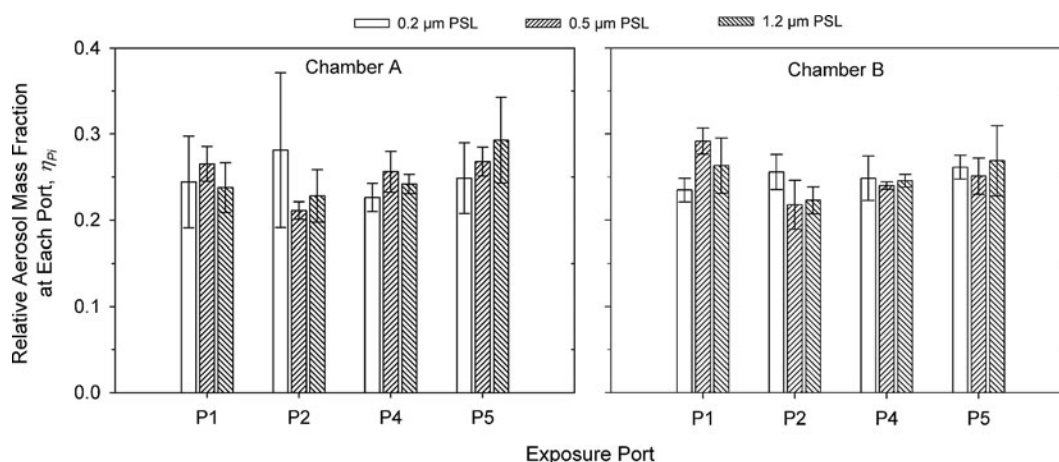


FIG. 2. Relative aerosol mass fraction at each port, η_{Pi} . PSL particles of different sizes were used. Means \pm SD from three independent measurements are shown.

when 0.5- μm PSL particles were used. However, no differences among the ports were detected when the data pooled for different particle sizes were analyzed. The average standard error of the η_{Pi} calculated from 12 data points for each chamber (four exposure ports and three different particle sizes) was 0.02 for Chamber A and 0.01 for Chamber B. Thus, the data presented above show that the test PSL particles were relatively uniformly distributed among the four exposure ports. Although the sampling regime did not mimic the inhalation–exhalation pattern of a test animal, the data indicate that the test animals would be presented with a similar concentration of the test aerosol.

We compared the particle mass collected at each exposure port with the total mass on all filters as described in Equation 1. The mean aerosol mass fraction for a single port, η_{Ti} , averaged across all ports and all particle sizes was $1.39\% \pm 0.30\%$ for Chamber A and $1.43\% \pm 0.24\%$ for Chamber B. These data indicate that approximately 6% of the total aerosolized particle mass that entered the distribution chamber was collected on four filters at exposure ports, and approximately 94% was collected at the exhaust filter.

As the next step, we investigated the size distribution of neutral liposomes, especially paying attention to its changes as a function of aerosolization time. Figure 3 shows the airborne liposome size distribution by number normalized to the size channel width at different aerosolization times, whereas Figure 4 shows the mean particle size in the air and liquid at different aerosolization times.

For freshly prepared liposomes, the mean particle size by number was approximately 130 nm and geometric standard deviation was 1.76. The mass median diameter of this size distribution was approximately 270 nm. As mentioned in Materials and Methods, in the initial experiments we also used an APS to check for the presence of particles too big to be detected by the SMPS. The measurements with the APS (results not included in Fig. 3) indicated that approximately 0.03% of all aerosolized particles were larger than 0.5 μm , and that they made up approximately 10% of the produced aerosol mass. If the APS data are added to the size distribution measured by the SMPS, then the median particle size by number and geometric standard deviation does not change, whereas the mass median diameter increases from

270 nm to approximately 285 nm. From these data, it was clear that the vast majority of the micrometer-sized droplets produced by the Collision nebulizer are desiccated by the time they reach the exposure points. As a result, we focused on the results from the SMPS measurements only.

According to Figure 3, the airborne particle size distribution as measured by the SMPS did not vary substantially over 60 min of aerosolization time. For comparison, experiments with certain bacteria have shown that the stress of continuous aerosolization by a Collision nebulizer results in fragmentation of the bacteria, which could be observed as an increased presence of particles smaller than the mean size of the bacteria.⁽⁴²⁾ Figure 3 does not show a change in airborne liposome size distribution, which indicates that the liposomes were not substantially damaged during their continuous aerosolization for 60 min. In fact, as shown in Figure 4, the mean particle diameters in liquid and in air showed little change over that time period. The mean liposome diameter in liquid (hydrodynamic diameter) varied from 127 to 135 nm, whereas their mean diameter in air (electrical mobility diameter) was 132 nm after 15 min of aerosolization and 131 nm after 60 min of aerosolization. The differences

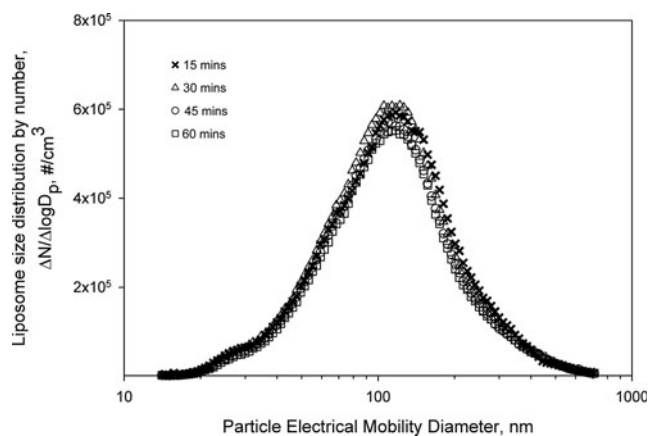


FIG. 3. Size distribution by number of airborne neutral liposomes as a function of aerosolization time. Means from three measurements are shown.

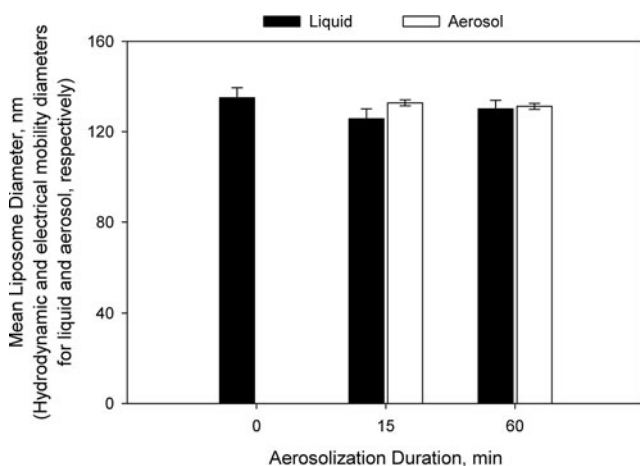


FIG. 4. Mean sizes of neutral liposomes as a function of aerosolization time. The data from liquid measurements represent mean hydrodynamic diameter, whereas the aerosol data represent electrical mobility diameter. Means \pm SD from three independent measurements are shown.

were not statistically significant for both media. The data in Figures 3 and 4 show that the employed DCS aerosolization method (Collison nebulizer) does not substantially affect the size distribution of liposomes as a function of aerosolization time and could be used to deliver the DCS to test animals without damaging the DCS.

The data presented above indicated that approximately the same aerosol mass concentration was delivered to each exposure port when the PSL particles were used, and that the neutral liposomes did not suffer substantial damage when aerosolized for up to 60 min. In the next step, we investigated the uniformity of liposome mass concentration across exposure ports. Here, the experimental conditions were the same as described above, and experiments were performed with Chamber A only. Figure 5 presents the two mass concentration factors, η_{Pi} and η_{Ti} , when neutral and cationic liposomes were aerosolized and sampled from the exposure ports. The relative aerosol mass fraction at each port, η_{Pi} , ranged from 0.22 to 0.29 for neutral liposomes and from 0.22 to 0.28 for cationic liposomes. The differences among ports in both cases

were not statistically significant. The fraction of the aerosol mass that entered the distribution chamber and was measured at each port, η_{Ti} , ranged from 0.01 to 0.014 for neutral liposomes and from 0.008 to 0.01 for cationic liposomes. There was no statistically significant difference among ports for both liposome types. The average mass fraction for neutral liposomes was 0.012 ± 0.001 , and for cationic liposomes it was 0.009 ± 0.001 ; according to the ANOVA test, the difference was statistically significant ($p < 0.05$). The difference might have been due to a different particle size. As measured in liquid, the average hydrodynamic diameter of neutral liposomes was approximately 130 nm, whereas that of cationic liposomes was approximately 80 nm. Nonetheless, as the relative mass distributions across ports were similar for both liposome types, the test animals would be presented a similar aerosol mass concentration.

In the next step of the study, we used the investigated exposure system to deliver liposomes containing DOX and ASO to test animals with lung tumors. Based on the experiments with fluorescent PSL particles and fluorescent liposomes as described above and inhalation conditions (25 mL/min for 10 min), we estimate that for DOX and ASO nebulizer concentrations of $50 \mu\text{g}/100 \mu\text{L}$ and $2.5 \mu\text{g}/100 \mu\text{L}$, respectively, each mouse would have inhaled approximately $0.28 \mu\text{g}$ of DOX and $0.014 \mu\text{g}$ of ASO per inhalation session. These concentrations take into account particle losses occurring in the exposure system. For i.v. injections, the doses were $50 \mu\text{g}$ of DOX and $2.5 \mu\text{g}$ of ASO per injection.

The retention of the drugs delivered by liposomes via inhalation to the animal lungs was compared with the retention of the same drugs delivered by i.v. injection, and the results are presented in Figure 6. It was found that when DOX and ASO were delivered by inhalation, their concentrations in the lungs were higher and they were retained for a much longer time period compared with the same parameters from i.v. injection (Fig. 6A and B). DOX and ASO were completely eliminated from the lungs in 2 days after i.v. injection (Fig. 6A and B, curves 1). In contrast, after inhalation delivery, more than 50% of the maximum DOX and ASO concentration was observed in the lungs after 2 days, and a substantial amount remained after 3 days (Fig. 6A and B, curves 2). The overall lung exposure calculated as area under the curve (AUC) was 5.8 to 6.5 times higher after inhalation

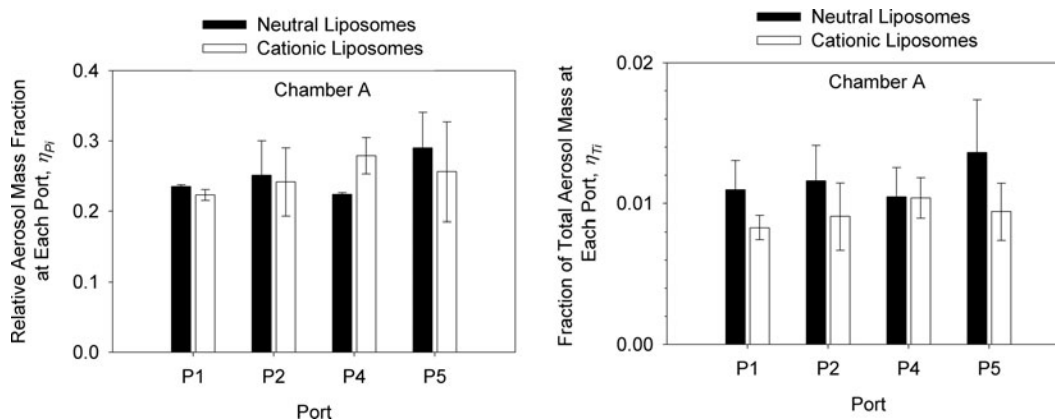


FIG. 5. Mass fractions of neutral and cationic liposomes at each exposure port. Means \pm SD from three independent measurements are shown.

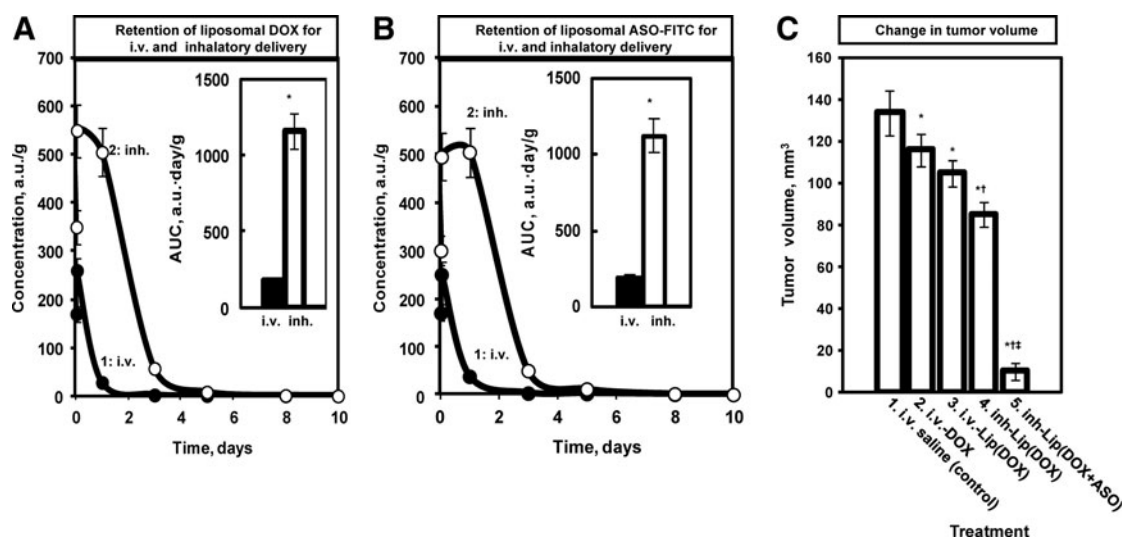


FIG. 6. Local inhalation codelivery of anticancer drug and suppressors of pump and nonpump resistance increases accumulation of active components in the lungs and enhances treatment of lung cancer. **(A, B)** Retention of liposomal DOX (A) and ASO (B) in lung tissues after i.v. injection (curve 1) and inhalation (curve 2). The fluorescence of DOX and ASO labeled with FITC was measured in the excised lungs within 10 days after completion of the treatment. Normalized per organ weight levels of fluorescence were plotted versus time, and an area under the curve (AUC) was calculated. Means \pm SD are shown. * $p < 0.05$ when compared with i.v. injection. **(C)** Antitumor activity of different liposomal formulations in mice bearing orthotopic model of human lung tumor. (1) i.v. injection of saline in untreated mice as control; (2) i.v. injection of free DOX (i.v.-DOX); (3) i.v. injection of liposomal DOX [i.v.-Lip(DOX)]; (4) inhalation of liposomal DOX [inh-Lip(DOX)]; and (5) inhalation of complex liposome-based DCS containing DOX and ASO targeted to MRP1 and BCL2 mRNA [inh-Lip(DOX+ASO)]. Means \pm SD are shown. * $p < 0.05$ when compared with untreated animals; † $p < 0.05$ when compared with i.v. injection of liposomal DOX [i.v.-Lip(DOX)]; ‡ $p < 0.05$ when compared with liposomal DOX delivered by inhalation [inh-Lip(DOX)].

delivery when compared with the i.v. injection (compare bars 1 and 2 in Fig. 6A and B). Therefore, the inhalation delivery of complex DCS substantially increased the overall exposure of the lung tissue to the anticancer drug and ASO. Similar data were obtained for liposomal delivery of DOX combined with siRNA (data not shown). This was despite the fact that the amount of drugs available for direct inhalation was estimated to be substantially lower compared with i.v. injection as described above.

We also observed that a higher retention of active drug components after inhalation delivery by liposomes enhanced the antitumor efficiency of the therapy compared with other delivery methods (Fig. 6C). The efficiency of the delivery method was analyzed by measuring the final tumor volume in mice treated seven times within a 24-day span with the following: (1) i.v. injection of saline as control; (2) i.v. injection of free DOX (i.v.-DOX); (3) i.v. injection of liposomal DOX [i.v.-Lip(DOX)]; (4) inhalation of liposomal DOX [inh-Lip(DOX)]; and (5) inhalation of complex liposomal carrier system (DCS) containing DOX and ASO targeted to MRP1 and BCL2 mRNA [inh-Lip(DOX+ASO)]. Although the i.v. treatment of mice bearing lung tumors using free DOX and liposomal DOX led to a moderate (but statistically significant) decrease in the total volume of lung tumor [i.v.-DOX and i.v.-Lip(DOX), respectively], a greater reduction in tumor volume was achieved by using inhalation treatment with liposomal DOX [inh-Lip(DOX)]. The reduction was statistically different from the control and treatments using i.v. injection of free DOX (i.v.-DOX) and liposomal DOX [i.v.-Lip(DOX)]. However, the greatest reduction in tumor volume was achieved

using inhalation administration of liposomal carrier system containing DOX and ASO targeted to MRP1 and BCL2 mRNA [inh-Lip(DOX+ASO)]. Here, the tumor volume decreased by more than 90% compared with the control treatment (Fig. 6C, compare bars 1 and 5). The tumor volume after this treatment was substantially and statistically significantly lower compared with other treatments. Thus, it seems that the suppression of cellular resistance by ASO targeted to BCL2 and MRP1 mRNA significantly enhanced the efficacy of liposomal DOX and allowed a substantial reduction in tumor volume to be achieved. Again, this was achieved by having a substantially lower amount of drugs available for direct inhalation compared with i.v. injection as described above. The observed results suggest a great potency of using complex liposomal DCS delivered via inhalation to treat lung cancer.

Conclusions

In this study, we successfully characterized a five-port nose-only exposure system for small animals and used the system for inhalation delivery of DCS containing an anticancer drug, ASO, and siRNA to experimental animals. Our experiments showed that the test PSL particles were relatively uniformly distributed among the four used exposure ports. The same result was achieved for neutral liposomes and cationic liposomes. Another important finding of the system characterization was that the liposomal DCS did not appear to be damaged by a continuous aerosolization of 60 min. The delivery of liposomes containing DOX and ASO to test animals with lung tumors using the investigated

system clearly indicated the superiority of inhalation delivery of the anticancer drugs together with pump and non-pump resistance suppressors compared with the i.v. injection or inhalation of anticancer drugs alone in liposomal form. First, when drugs were delivered by inhalation, the lungs received higher doses compared with i.v. injection of the same amount of drug. Second, a much greater reduction of tumor volume was observed after inhalation delivery of DOX and ASO targeted to MRP1 and BCL2 mRNA compared with i.v. injection or inhalation delivery of DOX alone in liposomes. Thus, our data suggest that the use of the investigated exposure system to deliver complex DCS containing anticancer drugs together with pump and nonpump resistance suppressors offers a superior method for lung cancer treatment compared with i.v. injections. At the same time, we recognize that further investigation of inhalation delivery of anticancer drugs, including dose-effect analysis, requires more rigorous study of inhaled and deposited drug dose, which will be the focus of our future investigations.

Acknowledgments

This work was supported in part by CA111766 NIH grant. We thank Dr. D.C. Reimer from Rutgers Lab Animal Services for his help with the development and implementation of an orthotopic mouse model of lung cancer.

Author Disclosure Statement

No conflicts of interest exist for any of the authors.

References

- Molina JR, Yang P, Cassivi SD, Schild SE, and Adjei AA: Non-small cell lung cancer: epidemiology, risk factors, treatment, and survivorship. *Mayo Clin Proc.* 2008;83:584–594.
- Parkin DM, Bray F, Ferlay J, and Pisani P: Global cancer statistics, 2002. *CA Cancer J Clin.* 2005;55:74–108.
- Minko T, Dharap SS, Pakunlu RI, and Wang Y: Molecular targeting of drug delivery systems to cancer. *Curr Drug Targets.* 2004;5:389–406.
- Pakunlu RI, Cook TJ, and Minko T: Simultaneous modulation of multidrug resistance and antiapoptotic cellular defense by MDR1 and BCL-2 targeted antisense oligonucleotides enhances the anticancer efficacy of doxorubicin. *Pharm Res.* 2003;20:351–359.
- Garbuzenko OB, Saad M, Pozharov VP, Reuhl KR, Mainelis G, and Minko T: Inhibition of lung tumor growth by complex pulmonary delivery of drugs with oligonucleotides as suppressors of cellular resistance. *Proc Natl Acad Sci USA.* 2010;107:10737–10742.
- Taratula O, Garbuzenko OB, Kirkpatrick P, Pandya I, Savla R, Pozharov VP, He H, and Minko T: Surface-engineered targeted PPI dendrimer for efficient intracellular and intratumoral siRNA delivery. *J Control Release.* 2009;140:284–293.
- Pakunlu RI, Wang Y, Saad M, Khandare JJ, Starovoytov V, and Minko T: *In vitro* and *in vivo* intracellular liposomal delivery of antisense oligonucleotides and anticancer drug. *J Control Release.* 2006;114:153–162.
- Saad M, Garbuzenko OB, and Minko T: Co-delivery of siRNA and an anticancer drug for treatment of multidrug-resistant cancer. *Nanomedicine.* 2008;3:761–776.
- Thompson DC: Pharmacology of therapeutic aerosols. In: AJ Hickey, (ed). *Pharmaceutical Inhalation Aerosol Technology (Drugs and Pharmaceutical Sciences)*, 2nd ed. Marcel Dekker, Inc., New York; pp. 29–59, 2003.
- Torchilin VP: Drug targeting. *Eur J Pharm Sci.* 2000;11:S81–S91.
- Anonymous. Inhaler for penicillin. *Lancet.* 1946;i:986.
- Melani AS: Inhalatory therapy training: a priority challenge for the physician. *Acta Biomed.* 2007;78:233–245.
- Valle MJ, González López F, and Sánchez Navarro A: Pulmonary versus systemic delivery of levofloxacin. The isolated lung of the rat as experimental approach for assessing pulmonary inhalation. *Pulm Pharmacol Ther.* 2008;21:298–303.
- de Jesús Valle MJ, López FG, Hurlé AD, and Navarro AS: Pulmonary versus systemic delivery of antibiotics: comparison of vancomycin dispositions in the isolated rat lung. *Antimicrob Agents Chemother.* 2007;51:3771–3774.
- de Jesús Valle MJ, Uranga NS, López FG, Hurlé AD, and Navarro AS: Disposition of linezolid in the isolated rat lung after systemic and pulmonary drug delivery. *J Antimicrob Chemother.* 2007;60:1074–1079.
- Gagnadoux F, Pape AL, Lemarie E, Lerondel S, Valo I, Leblond V, Racineux JL, and Urban T: Aerosol delivery of chemotherapy in an orthotopic model of lung cancer. *Eur Respir J.* 2005;26:657–661.
- Beck-Broichsitter M, Gauss J, Packhaeuser CB, Lahnstein K, Schmehl T, Seeger W, Kissel T, and Gessler T: Pulmonary drug delivery with aerosolizable nanoparticles in an *ex vivo* lung model. *Int J Pharm.* 2009;367:169–178.
- Borm PJ, and Kreyling W: Toxicological hazards of inhaled nanoparticles—potential implications for drug delivery. *J Nanosci Nanotechnol.* 2004;4:521–531.
- Nguyen J, Steele TW, Merkel O, Reul R, and Kissel T: Fast degrading polyesters as siRNA nano-carriers for pulmonary gene therapy. *J Control Release.* 2008;132:243–251.
- Ramesh R, Ito I, Saito Y, Wu Z, Mhashikar AM, Wilson DR, Branch CD, Roth JA, and Chada S: Local and systemic inhibition of lung tumor growth after nanoparticle-mediated mda-7/IL-24 gene delivery. *DNA Cell Biol.* 2004;23:850–857.
- Koshkina NV, Waldrep JC, Roberts LE, Golunski E, Melton S, and Knight V: Paclitaxel liposome aerosol treatment induces inhibition of pulmonary metastases in murine renal carcinoma model. *Clin Cancer Res.* 2001;7:3258–3262.
- Minko T, Stefanov A, and Pozharov V: Selected contribution: lung hypoxia: antioxidant and antiapoptotic effects of liposomal α -tocopherol. *J Appl Physiol.* 2002;93:1550–1560.
- Anabousi S, Bakowsky U, Schneider M, Huwer H, Lehr CM, and Ehrhardt C: *In vitro* assessment of transferrin-conjugated liposomes as drug delivery systems for inhalation therapy of lung cancer. *Eur J Pharm Sci.* 2006;29:367–374.
- Anabousi S, Kleemann E, Bakowsky U, Kissel T, Schmehl T, Gessler T, Seeger W, Lehr CM, and Ehrhardt C: Effect of PEGylation on the stability of liposomes during nebulisation and in lung surfactant. *J Nanosci Nanotechnol.* 2006;6:3010–3016.
- Garbuzenko O, Saad M, Betigeri S, Zhang M, Vetcher A, Soldatenkov V, Reimer D, Pozharov V, and Minko T: Intratracheal versus intravenous liposomal delivery of siRNA, antisense oligonucleotides and anticancer drug. *Pharm Res.* 2009;26:382–394.
- Schwendener RA: Liposomes in biology and medicine. In: WCW Chan, (ed). *Bio-Applications of Nanoparticles.* Springer, New York; pp. 117–128, 2007.

27. Samad A, Sultana Y, and Aqil M: Liposomal drug delivery systems: an update review. *Curr Drug Deliv.* 2007;4:297–305.
28. Allen TM, Williamson P, and Schlegel RA: Phosphatidylserine as a determinant of reticuloendothelial recognition of liposome models of the erythrocyte surface. *Proc Natl Acad Sci USA.* 1988;85:8067–8071.
29. Proffitt RT, Williams LE, Presant CA, Tin GW, Uliana JA, Gamble RC, and Baldeschwieler JD: Liposomal blockade of the reticuloendothelial system: improved tumor imaging with small unilamellar vesicles. *Science.* 1983;220:502–505.
30. Huang Y-Y, and Wang C-H: Pulmonary delivery of insulin by liposomal carriers. *J Control Release.* 2006;113:9–14.
31. Moss OR: Inhalation toxicology: sampling strategies related to control of exposure atmospheres. In: P Baron and K Willeke, (eds). *Aerosol Measurement: Principles, Techniques and Applications*, 2nd ed. Wiley-Interscience, New York; 2001.
32. Cannon WC, Blanton EF, and McDonald KE: The flow-past chamber: an improved nose-only exposure system for rodents. *Am Ind Hyg Assoc J.* 1983;44:923–928.
33. Port JL, Yamaguchi K, Du B, De Lorenzo M, Chang M, Heerdt PM, Kopelovich L, Marcus CB, Altorki NK, Subbaramaiah K, and Dannenberg AJ Tobacco smoke induces CYP1B1 in the aerodigestive tract. *Carcinogenesis.* 2004;25:2275–2281.
34. Vincent R, Bjarnason SG, Adamson IY, Hedgcock C, Kumarathasan P, Guénette J, Potvin M, Goegan P, and Bouthillier L: Acute pulmonary toxicity of urban particulate matter and ozone. *Am J Pathol.* 1997;151:1563–1570.
35. Saini D, Buller RM, Biris AS, and Biswas P: Characterization of a nose-only inhalation exposure system for ectromelia virus infection of mice. *Particulate Sci Technol.* 2009;27:152–165.
36. Stone RC, and Johnson DL: A note on the effect of nebulization time and pressure on the culturability of *Bacillus subtilis* and *Pseudomonas fluorescens*. *Aerosol Sci Technol.* 2002;36:536–539.
37. Mainelis G, Berry D, An HR, Yao MS, DeVoe K, Fennell DE, and Jaeger R: Design and performance of a single-pass bubbling bioaerosol generator. *Atmos Environ.* 2005;39:3521–3533.
38. Thomas RJ, Webber D, Hopkins R, Frost A, Laws T, Jayasekera PN, and Atkins T: The cell membrane as a major site of damage during aerosolization of *Escherichia coli*. *Appl Environ Microbiol.* 2011;77:920–925.
39. Han T, and Mainelis G: Design and development of an electrostatic sampler for bioaerosols with high concentration rate. *J Aerosol Sci.* 2008;39:1066–1078.
40. Dharap SS, Wang Y, Chandna P, Khandare JJ, Qiu B, Gunaseelan S, Sinko PJ, Stein S, Farmanfarmaian A, and Minko T: Tumor-specific targeting of an anticancer drug delivery system by LHRH peptide. *Proc Natl Acad Sci USA.* 2005;102:12962–12967.
41. Minko T, Kopecková P, and Kopecek J: Efficacy of the chemotherapeutic action of HPMA copolymer-bound doxorubicin in a solid tumor model of ovarian carcinoma. *Int J Cancer.* 2000;86:108–117.
42. Mainelis G, Willeke K, Baron P, Grinshpun SA, Reponen T, Górný RL, and Trakumas S: Electrical charges on airborne microorganisms. *J Aerosol Sci.* 2001;32:1087–1110.

Received on December 23, 2011
in final form, December 6, 2012

Reviewed by:
Wolfgang Kreyling
Theresa Sweeney

Address correspondence to:
Dr. Gediminas Mainelis
Department of Environmental Sciences
Rutgers, The State University of New Jersey
New Brunswick, NJ 08901

E-mail: mainelis@envsci.rutgers.edu